



ASSESSMENT OF DIFFERENT ELEVATION MASK ANGLES ON IONOSPHERIC AND TROPOSPHERIC DELAY ERROR BY USING REFRACTION MODELS

Mohamad .Eid A Shakour¹, Essam M.Fawaz², Mostafa H.A.Mohamed³

¹Demonstrator, Civil Department, Faculty of Engineering, Al- Azhar University, Cairo, Egypt.

²Professor, Civil Department, Faculty of Engineering, Al- Azhar University, Cairo, Egypt.

³Assistant Professor, Civil Department, Faculty of Engineering, Al- Azhar University, Cairo, Egypt.

Eid_Muhamad@yahoo.com, essamfawaz2001@gmail.com, Mostafa.hassan@azhar.edu.eg

المخلص العربي

يستخدم نظام تحديد المواقع العالمي (GPS) بشكل شائع لمراقبة التغيرات الزمنية والمكانية في سطح الأرض والمحيطات والغلاف الجوي. يعد استخدام نظام تحديد المواقع العالمي (GPS) لدراسة التباين في الغلاف الجوي السفلي للأرض أحد الأهمية الخاصة لهذه المراجعة. على الرغم من أن الأساليب والنماذج المستخدمة في تحليلات نظام تحديد المواقع العالمي (GPS) قد تقدمت بشكل ملحوظ خلال العقد الماضي، لا تزال هناك إمكانية للتطوير. تؤثر أخطاء النمذجة أيضاً على الارصاد عند زوايا ارتفاع منخفضة جداً. ستناقش في هذا البحث اكتشاف أخطاء الغلاف الجوي (خطأ تأخير أيونوسفير + خطأ تأخير التروبوسفير) عن طريق نماذج الانكسار Klobuchar و Hopfield تحت زوايا قناع ارتفاع مختلفة 12 درجة ، 14 درجة ، 16 درجة ، 18 درجة و 20 درجة من خلال معالجة الارصاد على برنامج Leica Geo Office (LGO) 8.4. يشير هذا البحث إلى قوة تأثير اختلاف زاوية قناع الارتفاع على أخطاء الأيونوسفير والتروبوسفير ويشير إلى أن أخطاء الغلاف الأيونوسفير والتروبوسفير تقل بشدة من (12 درجة إلى 14 درجة) و (18 درجة إلى 20 درجة) ولكنها مستقرة إلى حد ما من (14 ° إلى 16 °) ثم تقييم خطأ التأخير الأيونوسفير والتروبوسفيري عن طريق الاختبار الإحصائي T, في هذا البحث يظهر أيضاً أنه لا يوجد فرق كبير لزوايا القناع (14 درجة و 16 درجة) على خطأ تأخير الأيونوسفير والتروبوسفيري.

Abstract

The Global Positioning System (GPS) is commonly used to monitor temporal and spatial changes in the Earth's surface, oceans, and atmosphere. The use of GPS for studying variation in the Earth's lower atmosphere is of special importance to this review. Although the methods and models used in GPS analyses have advanced significantly over the last two decades, there is still potential for development. Modelling errors also affect observations at very low elevation angles. This paper will discuss the detection of errors of the atmosphere (ionospheric +tropospheric delay error) by refraction Klobuchar and Hopfield models under different elevation mask angle 12°,14°,16°,18°and 20°by processing on Leica Geo Office (LGO) software 8.4. This paper indicates the strength of the effect of elevation mask angle difference on ionospheric and tropospheric errors and refers to ionospheric and tropospheric errors reduce severely from (12° to 14°) and (18° to 20°) but fairly stable from (14° to 16°) Mask angles then evaluate ionospheric and

tropospheric delay error by T-statistical test in this paper also shows that there is no significant difference for (14° and 16°) Mask angles on ionospheric and tropospheric delay.

Keyword: Ionospheric error, Tropospheric error, Klobuchar model, Hopfield model and Mask angles.

1-INTRODUCTION

The propagation media has an impact on electromagnetic wave propagation at all frequencies, causing signal route bending, arrival modulation time delays, carrier phase advancements, scintillation, and other variations. The arrival timings of carrier modulations and carrier phases are the most important factors in GNSS positioning. A minimal delay is caused by geometric bending of the signal route, which is insignificant for elevation angles greater than 5°. Electromagnetic wave propagation across various atmospheric layers varies in a difficult way depending on location and time. The troposphere and ionosphere are the two primary areas of interest in the atmosphere. While GNSS position needs careful consideration of the effects of the environment on the observations, GNSS has emerged as a valuable technique for researching atmospheric advantages.

The ionosphere, which ranges from 50 km to 1,000 km in height, slows down the PRN code by the same amount as the carrier phase propagates near to the speed of light. The resultant delay is frequency-dependent since the ionosphere is a dispersive medium for microwaves. More specifically, the greater the delay, the lower the frequency. The cumulative electron content (TEC), which is dependent on the time of day/year, the solar cycle of 11 years, and the geographical location, affects the ionospheric delay in the GPS signal route. (El-Rabbany, 2006).

The greatest ionospheric delay occurs between 10 and 15 degrees north and south of the geomagnetic equator, when the Earth's magnetic field is horizontal. The LC3 eliminates the first-order 99.9% ionospheric impact while increasing the ionospheric maximum to 150 metres at low elevation angles. At a satellite elevation angle of 10, the second-order delay can produce a range bias of up to 4 cm, whereas the third-order effect is around 1–4mm. (Steigenberger, 2009).

The ionosphere is an atmospheric region of ionized gases that influences GPS signals. The carrier phase advance is a significant influence of the ionosphere examined. On the L1 and L2 frequencies, this effect is distinct, so the magnitude of the error can be determined. Five meters of a typical ionospheric error is (Skone, 1998). The tropospheric delay has two components. The hydrostatic (or "dry") component, which is dependent on the dry air gases in the atmosphere, accounts for around 90% of the delay. The remaining effect of the delay is accounted for by the "wet" component, which is dependent on atmospheric moisture content and contains substantial volumes of water vapour. (Emardson 1998, Dodson et al 1996). Because the wet component changes more geographically and temporally than the dry component, the errors in the wet component models are higher

than the errors in the dry component models. The dry component is usually referred to as "dry delay," while the wet component is referred to as "wet delay." (Davis et al, 1985).

Studies focused on enhancing ionospheric models Navigation, by using The Klobuchar model is the standard model for ionospheric GPS signal correction (Klobuchar, 1987; Klobuchar, 1991). This is a very specific model to account for the ionosphere's daily change. However, the accuracy of the Klobuchar model is very low and this model can typically eliminate only 60 %of the ionospheric total delay effect (Feess et al., 1987; Hofmann et al., 1997). Different models have been developed to improve positioning accuracy to achieve improved modeling accuracy for ionospheric delay or TEC, and different calibration methods have also been developed to reduce variations in hardware delay on L1 and L2 channels for both satellites and receivers. (Lanyi et al., 1988; Komjathy et al., 1996; Hu et al., 2004; Hoque and jakewski, 2007).

High-cost dual frequency receivers users could eliminate the first order of ionospheric delay by using a combination of ionosphere-free (IF) by combining various simultaneous frequency measurements. (Hofmann-Wellenhof, 2008), to correct for the ionospheric delay, a specific model must be applied by users of low-cost single-frequency receivers .Different types of models are produced which differ in input parameters, demand for computation, and accuracy. The Bent model (Newby and Langely, 1992) and the International Ionosphere Reference (IRI)-2000 model (Bilitza, 2001) are computationally intensive models that need frequent updating of significant quantities of solar flux and input data for Zurich sunspot counts.

For current ionospheric models based on reference stations or network, the time required to update the ionospheric grid and transmit the corrections to users will tag the actual ionospheric changes (Doherty P. H and Gendron, 1997).

Troposphere delay is primarily described in four models: Hopfield, Saastamoinen, Black, and Egnos. Troposphere delay is necessary for accurate GPS location. For a low elevation, the Hopfield, Saastamoinen, and Black models exhibit strong agreement with each other when using data from the GPS technical support Institution's (Crustal Dynamics Data Information System) CDDIS. The differences between the three models are minimal, and their accuracy is fairly good. The Hopfield, Saastamoinen, and Black models all have a maximum zenith troposphere delay error of less than 1 dm, although the Hopfield and Black models are more precise than the Saastamoinen model. The black variation might be considered the Enhanced Hopfield model form: The precision of the two models is equivalent at high elevations, but at low elevations, the Black model, elevation, shows to be more successful than Model Hopfield. The accuracy of the Egnos model is far lower than that of the Black, Hopfield, and Saastamoinen models. However, if real-time meteorological data is difficult to get in such part, the Egnos model may be a better option. (Wang ,Ji and Li.2009).

The dry delay, which is mainly due to atmospheric oxygen and nitrogen, is the other component of the tropospheric delay. The dry delay is 2.3 m at the zenith, while the wet

delay is 1-80 cm (Spilker, 1996). If the satellite gets near to the horizon, the total error increases more than 10 times (Seeber, 1993).

Globally, the monitoring of the ionosphere using GPS is available with the Establishing the GPS network of the International Global Navigation Satellite System Service (IGS). It can be used to provide, over time, global TEC mapping and its changes. Such products have been routinely supplied by IGS processing centers since 1996 (Schaer et al., 1996; Felten et al., 1999).

By reducing the elevation cut-off angle in connection with the global pressure and temperature model (GPT; Boehm et al. 2007), the high correlation between the zenith tropospheric delay and station height estimations can be significantly decreased. On the one hand, better mapping functions (GMF, VMF1) and improved stochastic models (observation weighting) are required for proper processing of low-elevation observations (Xiaoguang, 2013).

2- TROPOSPHEREIC ERROR: HOPFIELD MODEL

The Hopfield model is based on a relationship between dry refractivity at height h to that at the surface. The relationship was derived empirically on the basis of extensive measurements. This model referred to as a quartic model of refractivity profile (Misra, 2006), is

$$N_d(h) = N_{d0} \left(1 - \frac{h}{h_d}\right)^4 \dots\dots\dots (1)$$

Where h denotes the height above the antenna, N_{d0} is the dry refractivity at the surface, and h_d (≈ 43 km) is defined as the height above the antenna at which the dry refractivity is zero: $N_d(h_d) = 0$.

The Hopfield model for wet refractivity assumed a relationship similar to equation (1) though with less persuasive evidence

$$N_w(h) = N_{w0} \left(1 - \frac{h}{h_w}\right)^4 \dots\dots\dots (2)$$

Where N_{w0} is the wet refractivity at the surface and $h_w=12$ km from

$$\tilde{T} = 10^{-6} \int N(l) dl = 10^{-6} \int \{N_d(l) + N_w(l)\} dl = \tilde{T}_d + \tilde{T}_w$$

$$\tilde{T}_z = 10^{-6} \int \{N_d(h) + N_w(h)\} dh = \frac{10^{-6}}{5} [N_{d0} h_d + N_{w0} h_w] = \tilde{T}_{z,d} + \tilde{T}_{z,w}$$

Substituting expression for the dry and wet refractivities from

$$\{ N_d = 77.6 \frac{P}{T} \quad , \quad N_w = 3.73 * 10^5 \frac{e}{T^2} \}$$

$$\tilde{T}_{z,d} = 77.6 * 10^{-6} \frac{P_0}{T_0} \frac{h_d}{5} \dots\dots\dots (3)$$

$$\tilde{T}_{z,w} = 0.373 \frac{e_0}{T_0^2} \frac{h_w}{5} \dots\dots\dots (4)$$

The value of $\tilde{T}_{z,d}$ is 2.3 to 2.6 m at sea level, and gets lower as the altitude increase : about 2 m at Denver, Colorado, the mile-high city; and about 1 m atop a Himalayan peak. The Value of $\tilde{T}_{z,w}$ ranges from near-zero to 80 cm (millimetres in polar region, a few centimetres in deserts, and tens of centimetres in tropical areas).

The dry delay for the zenith direction ($\tilde{T}_{z,d}$) may be estimated with an accuracy of a few millimetres from accurate surface pressure measurements. The corresponding delay of depends upon the distribution of water vapour along the signal path, and can be highly variable (The mixing of the water vapour and dry air is complicated process depending upon the local weather conditions, and this distribution can change quickly). Wet delay $\tilde{T}_{z,w}$ models based on surface meteorological data are less precise, with average errors of 1 to 2 cm. use of average meteorological conditions rather than actual measurements introduces additional modelling error in both the dry and wet delay, and the total zenith delay error can be 5 to 10 cm(Misra 2006).

3-IONOSPHEREIC ERROR: KLOBUCHAR MODEL

The ionosphere is a layer of the Earth's atmosphere that exists between 50 and 2000 kilometres above the surface and is separated into layers by ionisation levels. The GPS ionospheric error is compensated by the satellite signal propagation delay acquired during the ionosphere's passage. The GPS ionospheric delay is proportional to the total electron content, or the number of electrons per unit area encountered during ionosphere crossing (TEC).It can be explained that relation between the GPS ionospheric delay in equation (5) and the TEC is expressed as in equation(6):

$$t_{iono} = \frac{40.5}{c \cdot f^2} \cdot \int_{h_1}^{h_2} N(h) \cdot dh \dots\dots\dots (5)$$

$$TEC = \int_{h_1}^{h_2} N(h) \cdot dh \dots\dots\dots (6)$$

Where:

t_{iono} ... Ionospheric delay of GPS.

c ... Light's velocity in free space.

f ... Radio wave frequency passing over the ionosphere (GPS radio signal).

$N(h)$... electron density in the ionosphere at a height of h above the Earth's surface.

TEC ... content of total electrons throughout the satellite ray route.

The total electron content that would be encountered if the satellite ray path attacked the ionosphere at the correct angle ($\pi/2$ radian) is generally taken into consideration using a normalised value of TEC. Because the angle of attack in this situation is different from $\pi/2$ radian, the right obliquity factor should be applied (Parkinson and Spilker, 1996). The geographic distribution of the ionospheric electron density $N(h)$ is shaped by a variety of factors, the majority of which are connected to processes occurring inside the ionosphere as a result of typically unpredictably solar and space weather impacts. Several trends in the $N(h)$ profile, however, have previously been observed. For illustrate, the daily distribution of the ionospheric delay has a different pattern, with a low and flat profile during the night

and a cosine-shaped distribution during the day. Around 14:00 local time, the day-time ionospheric delay reached its maximum level. Unfortunately, this pattern is more visible when the ionosphere is stable, as compared to when the ionosphere is highly disrupted.

The basic GPS ionospheric correction model, called after its developer John Klobuchar in equation (7), analyzes the aforementioned pattern (7):

$$t_{iono(Klobuchar)} = F \cdot (DC + A \cdot \cos(\frac{2 \cdot \pi \cdot (t - t_0)}{p})) \dots \dots (7)$$

Where:

$t_{iono(Klobuchar)}$... Time instant t [s] GPS ionospheric delay of a given day, according to Klobuchar.

F ... an oblique factor (related to satellite geometry).

DC ... time component at night (constant).

A ... the daily cosine component's amplitude.

$t_0 = 50200$ s (equal to 14.00 local time - peak time each day of $t_{iono(Klobuchar)}$).

P ... the daily cosine component's period.

The Klobuchar algorithm is explained in more detail elsewhere. The Klobuchar model has been shown to correct up to 70% of ionospheric delay, according to studies. During stabilized ionospheric condition, the Klobuchar model's success is significantly greater. Severe ionospheric disturbances, on the other hand, significantly change the daily ionospheric delay distribution, having a significant effect on the Klobuchar model's performance.

4-DATA COLLECTIONS

In this experimental work was established 8 points on the roof of the civil engineering department building, Al-Azhar a university, Cairo, Egypt where these points have located where no obstructions avoid satellite signal and have sky visibility and used **Trimble R4 GPS System** (dual frequency).

The Techniques of Surveying used are Fast Static technique with (session duration 30 minutes each point) for five tests in five days, and every test was changed the value of Mask Angle from GPS Controller Before observation and Mask Angle has chosen (12°, 14°, 16°, 18° and 20°).

Table 1 Days and Session Duration in different of mask angles

Test	Technique	Mask angle	Date	Session Duration (minute.)
Day 1	Fast Static	12 ⁰	27/08/2020	30
Day 2	Fast Static	14 ⁰	29/08/2020	30
Day 3	Fast Static	16 ⁰	30/08/2020	30
Day 4	Fast Static	18 ⁰	01/09/2020	30
Day 5	Fast Static	20 ⁰	02/09/2020	30

5-METHOD AND WORK PLAN

In Experimental Works, it is taken observations of 8 points by two- dual Frequency receivers Trimble R4 GPS. It is used the fast static technique with a session duration of 30 minutes for each point with an Elevation Mask angle 12⁰, 14⁰, 16⁰, 18⁰ and 20⁰. Observations file results from Trimble R4 GPS with .OT02 extension. So the result file is converted to 0.20o and 0.20n extension by (RINEX) format to input in LGO software. IGS final precise orbits were downloaded from CDDIS.NASA.GOV then Reference station Elat was selected as a control point to process observations from LGO software. The processing of observations was separated twice on each of mask angles of 12⁰, 14⁰, 16⁰, 18⁰ and 20⁰, the first processing was done without using correction models of refraction and the second processing was with using correction models (Tropospheric is Hopfield model and Ionospheric is Klobuchar Model). The difference between the two processing gives Tropospheric and Ionospheric delay Errors according to Hopfield model and Klobuchar Model in shown figure.1.and Table 2, shows general parameters that using in LGO software.

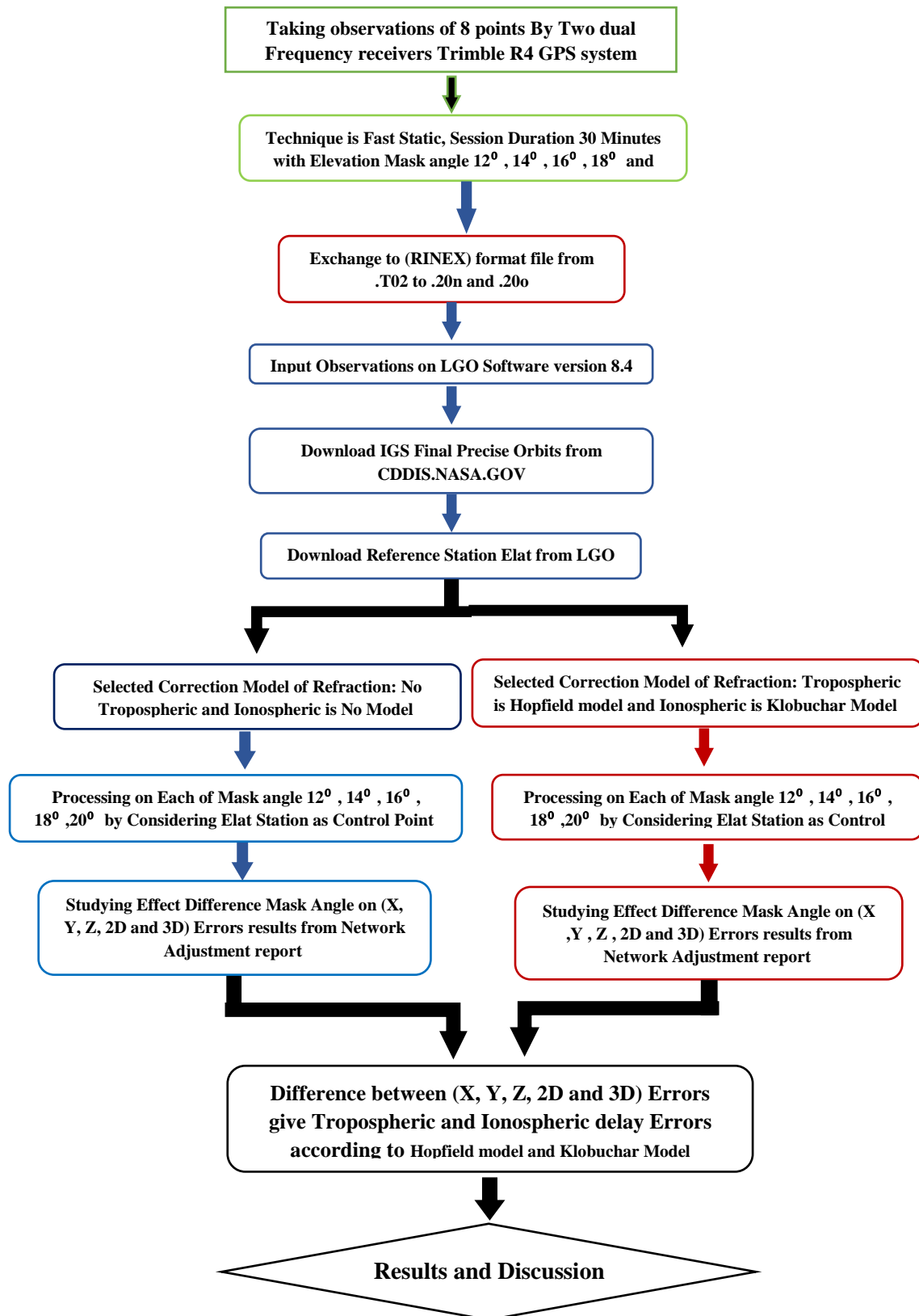


Figure 1. Show Method and Work Plan

Table 2. General parameters that using in LGO software to estimate errors result from (LGO Software 8.4)

General Parameters	Processing On LGO without Refraction Models	Processing On LGO with Refraction Models
Cut-off angle	12° - 14° - 16° -18° -20°	12° - 14° - 16° -18° -20°
Ephemeris type:	Precise	Precise
Solution type	Automatic	Automatic
GNSS type	GPS	GPS
Coordinate system name	WGS84	WGS84
Projection type	UTM Zone 36 North	UTM Zone 36 North
Disabled satellites
Strategy
Frequency	Automatic	Automatic
Fix ambiguities up:	80 km	80 km
Minimum float solution (static) duration:	300 sec	300 sec
Sampling rate	Use all	Use all
Tropospheric model	No Tropospheric	Hopfield model
Ionospheric model	No model	Klobuchar model
Stochastic modelling	Yes	Yes
Ionospheric activity	Automatic	Automatic
DOP values, Elevation /Azimuth	Yes	Yes
Storage rate for DOPs/Azimuth/Elevation	20% of data rate	20% of data rate
Residuals	No	No
Minimum time for common data	5 min	5 min
Maximum baseline length	500 km	500 km
Processing mode	All baselines	All baselines
Coordinate seeding strategy	Time	Time
Use float solutions as reference	No	No
Re-compute already computed baselines	No	No
Compute baselines between control triplets	No	No

6-RESULTS AND DISCUSSION

By using in LGO software to estimate errors result from (LGO Software 8.4).It is noticed that Ionospheric and Tropospheric delay Errors are minimal with increasing Elevation Mask angle as shown in tables 3 to 8 and fig 2.

Table 3. Compute Ionospheric and Tropospheric delay error at 12deg Mask angle by using Klobuchar and Hopfield models

12 degree	Errors with Refraction models			Errors without Refraction models			(Ionospheric Delay Klobuchar Model+Tropospheric Delay Hopfield Model) Errors m				
Points	X Error m	Y Error m	Z Error m	X Error m	Y Error m	Z Error m	ΔX Error m	ΔY Error m	ΔZ Error m	2D Error m	3D Error m
1	0.055	0.049	0.024	0.270	0.196	0.116	0.216	0.147	0.092	0.261	0.277
2	0.055	0.049	0.025	0.270	0.196	0.116	0.216	0.147	0.092	0.261	0.277
3	0.055	0.049	0.024	0.270	0.196	0.116	0.216	0.147	0.092	0.261	0.277
4	0.058	0.05	0.028	0.270	0.197	0.121	0.217	0.147	0.093	0.262	0.278
5	0.058	0.050	0.027	0.270	0.198	0.120	0.217	0.148	0.093	0.262	0.278
6	0.057	0.051	0.026	0.270	0.198	0.119	0.216	0.147	0.092	0.262	0.277
7	0.059	0.052	0.028	0.276	0.201	0.121	0.217	0.149	0.093	0.263	0.279
8	0.059	0.051	0.028	0.273	0.190	0.115	0.214	0.146	0.088	0.258	0.272
Mean	0.057	0.050	0.026	0.273	0.197	0.118	0.216	0.147	0.092	0.261	0.277
Max	0.059	0.052	0.028	0.276	0.201	0.121	0.217	0.149	0.093	0.263	0.279
Mini	0.055	0.049	0.024	0.270	0.190	0.115	0.214	0.146	0.088	0.258	0.272
St.Dev(m)										0.002	0.002

Table 4. Compute Ionospheric and Tropospheric delay error at 14deg Mask angle by using Klobuchar and Hopfield models

14 degree	Errors with Refraction models			Errors without Refraction models			(Ionospheric Delay Klobuchar Model+Tropospheric Delay Hopfield Model) Errors m				
Points	X Error m	Y Error m	Z Error m	X Error m	Y Error m	Z Error m	ΔX Error m	ΔY Error m	ΔZ Error m	2D Error m	3D Error m
1	0.081	0.092	0.041	0.154	0.190	0.082	0.073	0.098	0.041	0.123	0.128
2	0.092	0.108	0.047	0.160	0.196	0.085	0.069	0.088	0.038	0.111	0.118
3	0.080	0.091	0.039	0.153	0.190	0.082	0.074	0.099	0.043	0.123	0.130
4	0.080	0.091	0.039	0.153	0.190	0.082	0.074	0.099	0.043	0.123	0.130
5	0.132	0.143	0.073	0.263	0.265	0.169	0.132	0.121	0.096	0.179	0.203
6	0.082	0.091	0.041	0.154	0.189	0.083	0.073	0.099	0.041	0.122	0.129
7	0.082	0.092	0.041	0.154	0.189	0.082	0.072	0.098	0.041	0.122	0.128
8	0.081	0.091	0.040	0.154	0.189	0.082	0.073	0.099	0.042	0.122	0.129
Mean	0.089	0.100	0.045	0.168	0.200	0.094	0.080	0.100	0.048	0.128	0.136
Max	0.132	0.143	0.073	0.263	0.265	0.169	0.132	0.121	0.096	0.179	0.203
Mini	0.080	0.091	0.039	0.153	0.189	0.082	0.069	0.088	0.038	0.111	0.118
St.Dev(m)										0.021	0.027

Table 5. Compute Ionospheric and Tropospheric delay error at 16deg Mask angle by using Klobuchar and Hopfield models

16 degree	Errors with Refraction models			Errors without Refraction models			(Ionospheric Delay Klobuchar Model+Tropospheric Delay Hopfield Model) Errors m				
Point	X Error m	Y Error m	Z Error m	X Error m	Y Error m	Z Error m	ΔX Error m	ΔY Error m	ΔZ Error m	2D Error m	3D Error m
1	0.076	0.084	0.036	0.149	0.187	0.081	0.073	0.103	0.045	0.127	0.134
2	0.084	0.094	0.045	0.152	0.191	0.084	0.068	0.096	0.039	0.118	0.124
3	0.075	0.082	0.035	0.148	0.186	0.080	0.073	0.105	0.046	0.128	0.136
4	0.075	0.082	0.035	0.148	0.186	0.080	0.073	0.105	0.046	0.128	0.136
5	0.078	0.083	0.040	0.150	0.187	0.083	0.072	0.104	0.043	0.127	0.134
6	0.078	0.082	0.037	0.149	0.187	0.081	0.071	0.104	0.044	0.127	0.134
7	0.078	0.082	0.037	0.149	0.187	0.081	0.071	0.104	0.044	0.126	0.134
8	0.077	0.083	0.036	0.149	0.187	0.081	0.072	0.104	0.044	0.126	0.134
Mean	0.077	0.084	0.038	0.149	0.187	0.081	0.072	0.103	0.044	0.126	0.133
Max	0.084	0.094	0.045	0.152	0.191	0.084	0.073	0.105	0.046	0.128	0.136
Mini	0.075	0.082	0.035	0.149	0.186	0.080	0.068	0.096	0.039	0.118	0.124
St.Dev(m)										0.003	0.004

Table 6. Compute Ionospheric and Tropospheric delay error at 18deg Mask angle by using Klobuchar and Hopfield models

18 degree	Errors with Refraction models			Errors without Refraction models			(Ionospheric Delay Klobuchar Model+Tropospheric Delay Hopfield Model) Errors m				
Points	X Error m	Y Error m	Z Error m	X Error m	Y Error m	Z Error m	ΔX Error m	ΔY Error m	ΔZ Error m	2D Error m	3D Error m
1	0.040	0.041	0.019	0.108	0.128	0.058	0.068	0.088	0.0390	0.111	0.117
2	0.041	0.046	0.019	0.107	0.130	0.057	0.067	0.084	0.0390	0.107	0.114
3	0.039	0.039	0.017	0.107	0.128	0.057	0.068	0.089	0.040	0.111	0.118
4	0.039	0.039	0.017	0.107	0.127	0.057	0.0676	0.089	0.040	0.111	0.118
5	0.040	0.039	0.020	0.108	0.128	0.059	0.067	0.088	0.039	0.111	0.118
6	0.041	0.039	0.019	0.108	0.128	0.059	0.067	0.089	0.039	0.111	0.118
7	0.041	0.039	0.019	0.108	0.128	0.058	0.067	0.088	0.039	0.111	0.118
8	0.041	0.039	0.019	0.108	0.128	0.058	0.067	0.088	0.039	0.111	0.118
Mean	0.040	0.040	0.019	0.108	0.128	0.058	0.0675	0.088	0.040	0.111	0.117
Max	0.041	0.046	0.019	0.108	0.130	0.059	0.068	0.089	0.040	0.111	0.118
Mini	0.039	0.039	0.017	0.107	0.107	0.057	0.067	0.084	0.039	0.107	0.114
St.Dev(m)										0.001	0.001

Table 7. Compute Ionospheric and Tropospheric delay error at 20deg Mask angle by using Klobuchar and Hopfield models

20 degree	Errors with Refraction models			Errors without Refraction models			(Ionospheric Delay Klobuchar Model+Tropospheric Delay Hopfield Model) Errors m				
Point	X Error m	Y Error m	Z Error m	X Error m	Y Error m	Z Error m	ΔX Error m	ΔY Error m	ΔZ Error m	2D Error m	3D Error m
1	0.074	0.090	0.039	0.042	0.050	0.033	0.032	0.040	0.007	0.051	0.051
2	0.076	0.095	0.040	0.045	0.059	0.034	0.030	0.036	0.007	0.047	0.047
3	0.074	0.090	0.039	0.042	0.050	0.033	0.032	0.040	0.007	0.051	0.051
4	0.074	0.090	0.039	0.042	0.050	0.033	0.032	0.040	0.007	0.051	0.051
5	0.074	0.090	0.039	0.042	0.050	0.033	0.032	0.040	0.007	0.051	0.051
6	0.113	0.121	0.088	0.069	0.085	0.051	0.044	0.036	0.037	0.057	0.068
7	0.113	0.121	0.088	0.069	0.085	0.051	0.044	0.036	0.037	0.057	0.068
8	0.113	0.121	0.088	0.069	0.085	0.051	0.044	0.036	0.037	0.057	0.068
Mean	0.089	0.102	0.0560	0.0530	0.064	0.040	0.036	0.0380	0.018	0.052	0.055
Max	0.113	0.121	0.088	0.069	0.085	0.051	0.044	0.040	0.037	0.057	0.068
Mini	0.074	0.090	0.039	0.042	0.050	0.033	0.030	0.036	0.007	0.047	0.047
St.Dev(m)										0.004	0.009

Table 8. Mean 2D and 3D results from Ionospheric and Tropospheric delay at different Elevation Mask angles by using Klobuchar and Hopfield models

Elevation Mask angle	12°	14°	16°	18°	20°
Mean 2D Delay Error m	0.261	0.128	0.126	0.111	0.052
Mean 3D Delay Error m	0.277	0.136	0.133	0.117	0.055

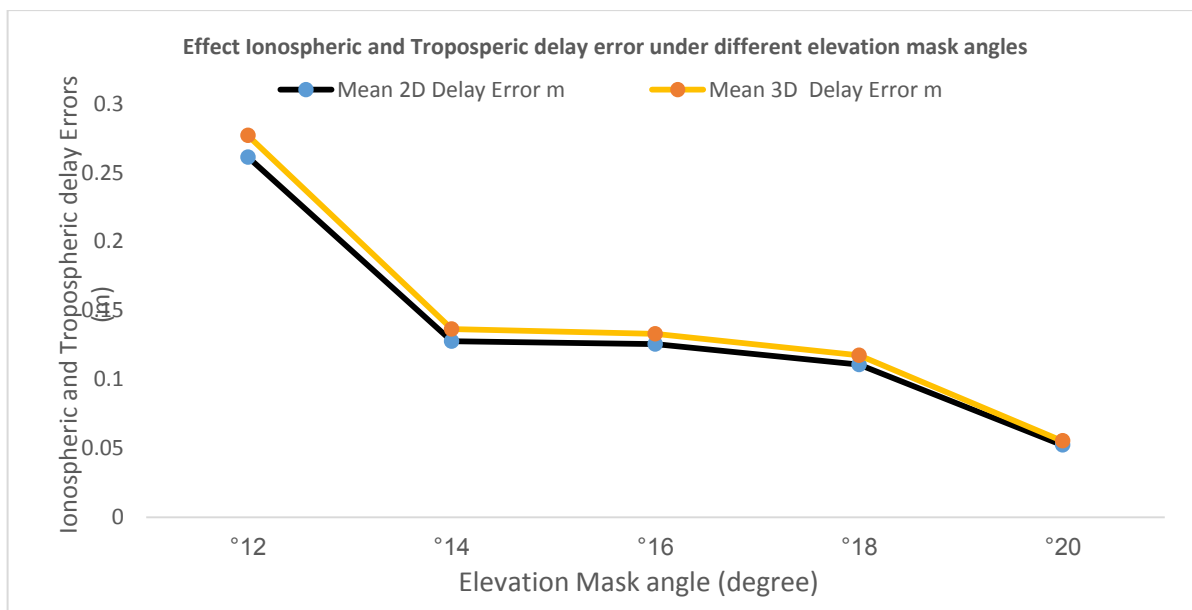


Figure 2. Relation between ionospheric and tropospheric errors with different of Mask angles

In fig 2 shows that decreasing of regression ionospheric and tropospheric errors is severe from (12° to 14°) and (18° to 20°) Mask angles, but decreasing of regression ionospheric and tropospheric errors is fairly stable from (14° to 16°) Mask angles, according to the minimum appropriate Satellite elevation mask angle (above the horizon) to eliminate the most noise in the GNSS signals due to atmospheric delay and refraction or even multipath conditions is 10° to 20° for Real-Time Positioning surveying (Henning,2011). By applying the T-statistical test on 5 tests, the results are shown in Table 9.

Table 9. Using T-calculated Statistical values results from 5 testes for 2D and 3D Errors (ionospheric+tropospheric) delay.

T-calculated values results from 5 testes for 2D Error.					
Mask angle	12°	14°	16°	18°	20°
12°	0.000	17.971	106.654	210.675	149.890
14°	17.971	0.000	0.277	2.290	10.024
16°	106.654	0.277	0.000	11.965	42.413
18°	210.675	2.290	11.965	0.000	42.558
20°	149.890	10.024	42.413	42.558	0.000
T-calculated values results from 5 testes for 3D Error.					
Mask angle	12°	14°	16°	18°	20°
12°	0.000	14.626	95.529	187.163	67.520
14°	14.626	0.000	0.361	1.993	8.045
16°	95.529	0.361	0.000	11.068	22.402
18°	187.163	1.993	11.068	0.000	19.170
20°	67.520	8.045	22.402	19.170	0.000

-T-statistical parameters: Degree of freedom=7, confidence level 95% so t-crti =1.894 from T-table

There is no significant difference for (14°and 16°) Mask angle on ionospheric delay and tropospheric delay. There is a significant difference for (12°, 18° and 20°) Mask angle on ionospheric delay and tropospheric delay.

7-CONCLUSION

The most common sources of satellite navigation errors are ionospheric and tropospheric delay errors. Successfully overcoming the GPS ionospheric and tropospheric delay increase the positioning accuracy of satellite navigation systems, so base on the previous results of this paper by using refraction (Klobuchar for the ionospheric and Hopfield tropospheric delay) models under different elevation mask angle 12°, 14°, 16°, 18° and 20° to compute and evaluate ionospheric delay error and tropospheric delay error.

1-Ionospheric and Tropospheric delay Errors are minimal with increasing Elevation Mask angle, in addition decreasing ionospheric and tropospheric errors is severe from (12° to 14°) and (18° to 20°) Mask angles, but ionospheric and tropospheric errors are fairly stable from (14° to 16°) Mask angles.

2- There is no significant difference for (14°and 16°) Mask angle on ionospheric delay and tropospheric delay.

3-There is a significant difference for (12°, 18° and 20°) Mask angle on ionospheric delay and tropospheric delay so the optimised Elevation mask angle is 14° to 16°.

8-REFERENCES

- Bilitza, D. (2001).** International Reference Ionosphere 2000. *Journal of Radio Science*, Vol. 36, No. 2, pp. 261-275
- Boehm, J., Heinkelmann, R., & Schuh, H. (2007).** Short note: A global model of pressure and temperature for geodetic applications. *Journal of Geodesy*, 81(10), 679–683. doi:10.1007/s00190-007-0135-3.
- Davis, J.L., T.A.Herring, I.I., Shapiro, A.E.E. Rogers, and G. Elgered (1985),** "Geodesy by radio interferometry: Effects of atmospheric modeling errors on estimates of baseline length", *Radio Science*, Vol.20, No. 6, pp. 1593-1607
- Dodson A.H., P.J. Shardlow, L.C.M. Hubbard, G. Elgered, and P.O.J. Jarlemark (1996),** "Wet Tropospheric effects on precise relative GPS height determination", *Journal of Geodesy*, No. 70, No. 4, pp. 188-202
- Doherty P. and Gendron P. J. (1997),** "The Spatial and Temporal Variation in Ionospheric Range Delay", *Proceedings of ION GPS-97*, Kansas City, Missouri USA, Vol. 1, pp. 231-240.
- El-Rabbany, A. (2006).** *Introduction to GPS: The Global Positioning System (2nd ed.)*. Norwood: Artech House.
- Emardson T.R. (1998),** "Studies of atmospheric water vapor using the Global Positioning System", Technical report No. 339, Chalmers University of Technology
- Feess W and Stephens S.(1987).** Evaluation of GPS ionospheric time delay model, *IEEE Trans. Aerospace and Electronic System*, Vol 23, No 3, pp 332- 338.
- Feltens, J., Schaer, S.(1999).** A combined IGS Ionospheric Product, IGS 1998 Annual Report, JPL Publication 400-839.
- Henning W., (2001),** "User Guidelines for single Base Real Time GNSS Positioning", National Oceanic and Atmospheric Administration, National Geodetic Survey , 138 pages
- Hofmann-Wellenhof, B., H. Lichtenegger and J. Collins.(1997).** *Global Positioning System: theory and practice*, Springer-verlag, wein, New York, fourth revised edition.
- Hofmann-Wellenhof B., Lichtenegger H., Wasle E. (2008).** *GNSS—global navigation satellite systems — GPS, GLONASS, Galileo, and more*. Springer, Vienna. doi:10.1007/978-3-211-73017-1
- Hoque M.M. and Jakowski J.(2007a).** Mitigation of higher order ionospheric effects on GNSS users in Europe, *GPS Solution*, doi: 10.1007/s 10291-007-0069-5
- Hu C, Chen W., Gao S., Chen Y, Ding X, Kwok S.(2004).** Absolute ionospheric delay estimation based on GPS PPP and GPS active network, *International Symposium on GPS/GNSS 2004*, Sydney, 6-8 Dec. 2004.
- Klobuchar J.(1987).** Ionospheric time-delay algorithm for single frequency GPS users, *IEEE Trans. Aerospace and Electronic Systems*. Vol 23 No.3, pp 325- 332.

- Klobuchar J(1991).** Ionospheric effects on GPS, GPS World, April 1991, pp 48-51.
- Komjathy, A., and R.B. Langly.(1996)** An Assessment of predicted and Measured Ionospheric Total Electron Content using a Regional GPS Network, ION GPS-96.
- Lanyi, et al.(1988).** A comparison of mapped and measured total ionospheric electron content using global positioning system and beacon satellite observations. Radio Science Vol 23
- Newby, S.P. and R.B. Langley (1992).** Three alternative empirical ionospheric models -- Are they better than the GPS Broadcast Model. Proceedings of the 6th International Geodetic Symposium on Satellite Positioning, Columbus, OH, 17–20 March, pp. 240–244.
- Misra P, Enge P (2006)** Global Positioning System: signals, measurements, and performance. Ganga-Jamuna Press, Massachusetts.
- Parkinson, B. W., J. J. Spilker, Jr. (1996).** Global Positioning System: Theory and Applications. AIAA. Washington, DC.
- Steigenberger, P., Boehm, J.,& Tesmer, V. (2009).** Comparison of GMF/GPT with VMF1/ECMWF and implications for atmospheric loading. Journal of Geodesy, 83(10), 943–951. doi:10.1007/s00190-009-0311-8.
- Skone, S. (1998).** Wide Area Ionospheric Grid Modelling in the Auroral Region. PhD thesis, Department of Geomatics Engineering, University of Calgary, December.
- Spilker, J. (1996b).** Global Positioning System: Theory and Applications, Chapter 13: Tropospheric Effects on GPS. Volume 163, Progress in Astronautics and Aeronautics, pp. 517-546.
- Seeber, G. (1993).** Satellite Geodesy Foundations, Methods, and Applications. Published by Walter de Gruyter, pp. 291-295.
- Schaer, S., G. Beutler, M. Rothacher, and T. A. Springer.(1996).** Daily Global Ionosphere Maps Based on GPS Carrier Phase Data Routinely Produced by the CODE Analysis Center, in Proceedings of the IGS Analysis Center Workshop, Silver Spring, Maryland, USA., edited by R. E. Neilan et al., pp. 181-192, IGS Central Bureau, JPL, Pasadena, California, USA, March 19-21, 1996
- (Wang Xinlong, Ji Jiaying and Li Yafeng.2009)** The applicability analysis of troposphere delay error model in GPS positioning Aircraft Engineering and Aerospace Technology: An International Journal 81/5 (2009) 445–451
- Xiaoguang Luo (2013).** "GPS Stochastic Modelling Signal Quality Measures and ARMA Processes" Doctoral Thesis accepted by the Karlsruhe Institute of Technology, Karlsruhe, Germany.